SSRG International Journal of Civil Engineering
ISSN: 2348-8352/ https://doi.org/10.14445/23488352/IJCE-V13I8P127

Volume 13 Issue 8, 450-468, August 2026

Original Article

Multi-Objective Optimization of GGBS Blended Pervious Concrete: Coupling Mechanical Strength, Permeability, and Water Purification via Microstructure Control

Urmila R. Kawade[1], Deepak G B[2*], Anand B[3], Lakshmi H S[4], Pradeep C R[5], Prashant Sunagar[6], Jagadish Vengala[7]

[1]*Department of Civil Engineering, Dr.V.V.Patil COE, Ahilyanagar, Maharashtra, India.*
[2]*Department of Civil Engineering, Dayananda Sagar Academy of Technology and Management, Bengaluru, Karnataka, India.*
[3]*Department of Civil Engineering, Jawaharlal Nehru New College of Engineering, Shivamogga, Karnataka, India.*
[4]*Department of Civil Engineering, M S Ramaiah institute of technology, Bengaluru, Karnataka, India.*
[5]*Department of Civil Engineering, Bangalore Institute of Technology, Bengaluru, Karnataka, India.*
[6]*Department of Civil engineering, Jyothy Institute of Technology, Bengaluru, Karnataka, India.*
[7]*Department of Civil Engineering, Prasad V. Potluri Siddhartha Institute of Technology (Autonomous), Kanuru, Vijayawada, Andhra Pradesh, India.*

[2*]*Corresponding Author : deepakgb@dsatm.edu.in*

Received: 16 March 2026 Revised: 27 May 2026 Accepted: 16 July 2026 Published: 31 August 2026

Abstract *- This study extends the design space of pervious concrete with respect to strength, drainage, and water purification using a multi-objective optimization approach. GGBS was used as a partial cement replacement (15–45%) across four no-fines coarse-aggregate gradations and assessed for compressive strength (accelerated, 7-day, and 28-day), constant and falling head permeability, and water filtration. The optimal formulation - a 60:40 blend by mass of the 16–10 mm and 10–4.75 mm coarse-aggregate fractions, with 30% GGBS - develops a compressive strength of 11.78 MPa at 7 days rising to 18.83 MPa at 28 days, together with a measured permeability coefficient of 2.0 mm/s and removals of 23.8% of dissolved solids and 10.2% of suspended solids. Microstructural images from SEM and porosity specifications indicate that slag modification densifies the interfacial transition zone without impeding drainage. Structure–property relationships align with previous studies indicating the presence of a design space with an optimal strength target for multifunctional properties. This evidence demonstrates that microstructural optimization via slag enables simultaneous structural and environmental performance, thereby promoting the use of pervious concrete in urban infrastructures.*

Keywords *- Pervious concrete, Multi-objective optimization, Aggregate gradation, Water purification, Permeability.*

1. Introduction

Transport of fluids through cementitious materials controls their long-term performance, durability, and function. Conventional concrete is designed to be dense and impermeable to prevent fluid ingress, and the deterioration processes it induces. Pervious concrete is a designedly permeable cementitious material, with its interconnected pore structures facilitating the rapid transport of fluids through its matrix. By enabling precipitation and runoff to percolate through the material rather than the air above, it establishes its functionality as a pervious concrete material: it combines ordinary structural properties with hydraulic function. Recent interest in pervious concrete has shifted from its original view as a purely hydraulic pavement material to investigating its potential as a multifunctional cementitious material. By omitting or severely reducing fine aggregates in its design, pervious concrete has 15–30% void fractions of connected pores, leading to its interconnected and highly permeable pore structure; however, this also leads to its corresponding low mechanical strength relative to standard concrete. Improving these mechanical properties has been studied by optimizing the gradation of aggregates, paste volume, and water: binder ratios, and the use of Supplementary Cementitious Materials (SCMs) and chemical admixtures.

In the pervious concrete system, the same pore structure that allows for the infiltration of stormwater into the sub-surface substrates also reduces the strength of pervious concrete. The engineering of pervious concrete systems requires a balance to be struck between the permeability of concrete and its strength. Portland cement replacement with GGBS is often employed in conventional concrete systems to reduce the amount of cement required to achieve high strength concrete while also reducing the carbon footprint of the concrete systems. In pervious concrete systems, GGBS can have a similar role as it can increase the strength of pervious concrete systems while also reducing the amount of cement that is required to set those pervious concrete systems. However, most existing studies on pervious concrete systems have considered each of these variables as separate design considerations within pervious concrete systems, and little study has been done on how to simultaneously optimize the strength, permeability, and water quality of pervious concrete systems using GGBS. Accordingly, the problem to be solved by the present study is how to formulate a pervious concrete system that utilizes both gradation of the aggregates and the addition of GGBS to satisfy the requirements of strength, permeability, and water quality.

While these techniques have shown promise in revealing the degree to which mechanical properties and permeability can be improved, improvements in one property do not necessarily result in the same outcome for the other, reinforcing the notion of a trade-off when designing pervious concrete in such less-dense systems: pore connectivity affects mechanical load transfer through the aggregate-binder skeleton of the system. The schematic pervious concrete pavement system is shown in Figure 1.

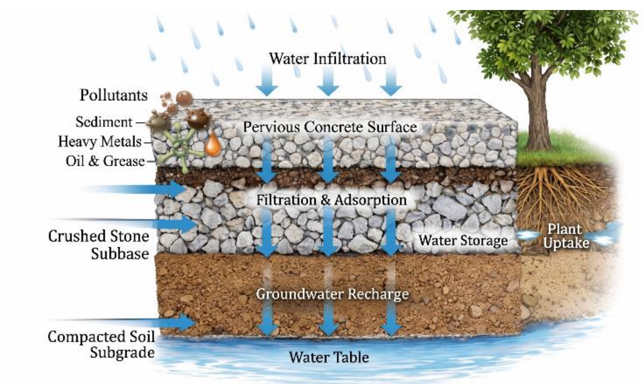

Fig. 1 Schematic of pervious concrete pavement system (Surface layer-subbase-subgrade; infiltration path)

The novelty of this work is in integrating three different aspects of pervious concrete that are usually evaluated separately in pervious concrete: its resistance to mechanical loads, hydraulic conductivity, and preliminary water purification. While many existing pervious concretes studies evaluate only the compressive strength of pervious concrete or their permeability, this study evaluates the effect of GGBS replacement levels, along with aggregate gradation, on pervious concrete's strength, permeability, and water purification capabilities. Furthermore, by utilizing indicators of water purification, such as pH, TDS, and TSS, this study provides an effective means of evaluating pervious concrete for both drainage and water purification applications. Thus, this study provides a method of selecting the best mix of GGBS-blended pervious concrete for pavements that require low volumes of water to flow through the pervious concrete.

2. Review of Literature

Pervious concrete is a type of building material that helps to manage stormwater through infiltration into the ground and purification of that infiltrated water. However, pervious concretes contain voids within their structure that contribute to both their high permeability but also reduce their strength [1, 2]. Ground Granulated Blast-Furnace Slag (GGBS) is a type of industrial by-product that is often blended into pervious concretes to increase their strength and reduce their carbon footprint [3, 4]. The addition of GGBS to pervious concretes contributes to the formation of a densified concrete structure whose properties are still controlled by the pervious macropores that enable water to infiltrate the concrete and become purified.

Pervious concrete is an environmentally beneficial pavement material characterized by an interconnected pore network that allows stormwater infiltration, reduces surface runoff, and supports groundwater recharge. However, its hydraulic function creates an inherent conflict between mechanical strength and permeability. Increasing interconnected porosity generally improves water flow but reduces the effective load-bearing area, resulting in lower compressive, tensile, and flexural strength [1-4]. Consequently, pervious concrete mixture design requires simultaneous consideration of structural and hydraulic performance rather than optimization of either property independently.

Ground-Granulated Blast-Furnace Slag (GGBS) has received considerable attention as a partial replacement for ordinary Portland cement because it can reduce cement consumption and associated carbon emissions while improving the later-age performance of concrete [1, 5]. The performance of GGBS-blended pervious concrete nevertheless depends strongly on replacement level, binder rheology, aggregate characteristics, compaction, curing conditions, and target porosity. Experimental studies indicate that moderate GGBS replacement can maintain or improve mechanical performance without causing an unacceptable reduction in permeability [2, 3, 6].

Oinam et al. reported that pervious concrete containing approximately 60% GGBS achieved compressive strength, porosity, and permeability comparable to those of the control mixture [2]. However, complete replacement of cement with activated GGBS reduced strength because of inadequate binder adhesion and non-uniform paste distribution. Seeni et al. observed improvements in compressive, splitting tensile, and flexural strength at GGBS replacement levels of up to approximately 40% [3]. In contrast, Sathe and Dandin identified approximately 20% GGBS as the most favourable level for compressive strength in their permeable concrete mixtures [6]. These differences demonstrate that a single universal optimum GGBS percentage cannot be established because performance is also controlled by water-to-binder ratio, aggregate grading, paste volume, activator type and curing regime.

Microstructural modification is the principal mechanism through which GGBS influences concrete performance. The latent hydraulic reaction of GGBS consumes calcium hydroxide and promotes the formation of additional calcium-silicate-hydrate and calcium-aluminosilicate-hydrate phases [5, 7]. These products refine the capillary pore structure, densify the interfacial transition zone and improve paste–aggregate bonding [7-10]. Such changes generally enhance mechanical strength and resistance to aggressive substances. Nevertheless, excessive microstructural densification can obstruct the interconnected macropores required for water transmission through pervious concrete.

Different characterization techniques provide complementary information about this pore system. Scanning electron microscopy and energy-dispersive spectroscopy reveal hydration products, microcracks and interfacial bonding, whereas mercury-intrusion porosimetry and nuclear magnetic resonance characterize smaller pore fractions [7, 8]. X-ray computed tomography is particularly useful for pervious concrete because it provides three-dimensional information regarding pore connectivity, distribution, tortuosity and paste segregation [2]. Therefore, total porosity alone should not be used to predict performance. Mixtures with similar porosity may exhibit considerably different permeability because of differences in pore size, connectivity and tortuosity.

The addition of fibres, viscosity-modifying agents and other admixtures further influences the mechanical–hydraulic balance. Yan et al. found that hydroxypropyl methylcellulose could improve binder stability and reduce uncontrolled paste drainage, whereas fibres and fine GGBS particles could occupy or obstruct interconnected voids when used excessively [4]. Improvements in aggregate–paste bonding may consequently increase strength but simultaneously decrease permeability. Water-to-binder ratio and superplasticizer dosage also affect paste coating, workability and water absorption, indicating that rheological control is essential for producing a uniform and stable pore network [11].

GGBS generally improves durability by reducing capillary porosity, chloride penetration, water absorption and ion transport [5, 9, 12, 13]. However, reduced transport through the cementitious matrix should not be confused with the designed macroscopic permeability of pervious concrete. An effective mixture should contain a dense and durable binder surrounding the aggregates while retaining continuous macropores between aggregate particles. Carbonation may also remain a concern because high GGBS replacement can reduce the alkalinity reserve of the binder [9, 10].

Clogging is another important long-term consideration. Fine sediments can accumulate within interconnected pores and gradually reduce infiltration capacity. El-Hassan and Kianmehr demonstrated that a substantial proportion of lost permeability could be recovered through water flushing, suggesting that pore accessibility and maintenance procedures are as important as initial permeability [1]. Thus, optimization should consider long-term permeability and recoverability rather than only initial laboratory measurements.

Although pervious concrete is frequently associated with stormwater-quality improvement, direct research on pollutant removal by GGBS-blended pervious concrete remains limited. The refined hydration products and altered surface chemistry produced by GGBS may support adsorption, precipitation and immobilization of certain pollutants. Its interconnected pore network may also facilitate filtration and increase contact between contaminated water and reactive cementitious surfaces. However, the reviewed studies do not provide sufficient direct evidence concerning the removal of phosphorus, nitrogen, heavy metals, hydrocarbons, microorganisms or microplastics. The effects of contaminant saturation, desorption, carbonation, leaching and repeated storm events also remain uncertain.

Existing optimization studies primarily examine strength, porosity, permeability or individual durability indicators. Comprehensive multi-objective optimization involving mechanical strength, hydraulic conductivity, clogging resistance, water purification, embodied carbon and cost remains scarce. Future studies should combine experimentally measured microstructural descriptors with response-surface methods, machine-learning models and Pareto-based algorithms such as NSGA-II. Such an approach would identify several technically feasible trade-off mixtures instead of presenting one mixture as universally optimal.

In conclusion, moderate GGBS replacement can improve the strength, durability and environmental performance of pervious concrete when paste rheology and pore connectivity are properly controlled. The critical design objective is to densify the binder and interfacial transition zone without blocking the interconnected macropore network. Current evidence adequately explains the mechanical–hydraulic trade-off, but direct evidence on water-purification performance remains insufficient. Future investigations should therefore integrate mechanical, permeability, microstructural, pollutant-removal and long-term durability measurements within a genuine multi-objective optimization framework.

The effect of silica fume and GGBS on the engineering properties of recycled-aggregate pervious concrete was studied by Bai et al. [14]. Those authors evaluated several blends of pervious concrete that incorporated silica fume, GGBS, and recycled coarse aggregate. The study assessed the effects of these additions upon compressive strength, porosity, permeability coefficient, and Cantabro abrasion resistance. The use of silica fume and GGBS led to an increase in compressive strength and abrasion resistance, yet a decrease in porosity and hydraulic conductivity. The blend containing 7% silica fume and 20% GGBS exhibited the highest compressive strength of that series (28.9 MPa at 28 days) together with the lowest permeability coefficient (1.2 mm/s) and the lowest Cantabro mass-loss rate (12.1%). The authors attributed the increase in strength and abrasion resistance to the densification of the hydraulic cement paste and the interfacial zones between aggregate particles. However, the concretes evaluated by Bai et al. [14] incorporated both recycled coarse aggregate and a ternary system of cementitious materials, while the present investigation utilizes only an OPC-GGBS system and examines the effects of GGBS replacement and aggregate size distribution alone.

Sha et al. investigated the effects of water-to-binder ratio, porosity and pore size on pervious concrete's mechanical and hydraulic performance. The size of the pores within pervious concrete was measured using image binarization techniques, and the d60 pore size represented the size of the concrete's core pores. As the porosity of pervious concrete was increased from 12% to 27%, the permeability coefficient increased by 120.41-233.33%, yet the compressive strength of pervious concrete decreased by 34.09-39.29%. The study found that compressive strength was negatively correlated with both the porosity and pore size within pervious concrete, while permeability exhibited a nonlinear polynomial relationship with both variables. Although porosity alone was found to not be sufficient to ensure the hydraulic performance of pervious concrete, pore size must also be considered. Nevertheless, the study did not investigate the effects of using GGBS in pervious concrete to improve water quality.

Sathe and Dandin produced pervious concretes that contained 5-25% fly ash or GGBS by weight of cement with water-to-binder ratios between 0.30 and 0.45. Testing included evaluation of compressive, splitting-tensile and flexural strength, density, porosity, falling-head permeability, sulfate resistance, SEM and XRD analyses. The addition of either fly ash or GGBS to pervious concrete can increase its strength; however, the best results were achieved with 15% replacement of cement with fly ash or 20% replacement of cement with GGBS. Additionally, both pozzolanic materials reduced the concrete's porosity and permeability and the correlations between these variables and strength.

Yuan et al. investigated the influence of different mineral admixtures on pervious concrete's mechanical and hydraulic performance. The influences on pervious concrete's microscopic characteristics were also evaluated. While related to the analysis of pervious concrete's SEM images, this study did not investigate the relationship between strength, permeability and water purification through pervious concrete.

Most of the existing studies show that supplementary cementitious materials improve the paste and interfacial transition-zone quality of pervious concrete. This leads to an increase in the compressive strength and abrasion resistance of pervious concrete but a decrease in the connected porosity and permeability. However, studies on the topology of pores within pervious concrete show that the hydraulic performance of pervious concrete also depends on the size of the pores within the concrete.

Most of the studies that have tried to find the best mix of pervious concrete have mainly considered the mechanical properties of pervious concrete, such as its strength, permeability, durability, cost, or environmental impact. Few studies have considered the performance of pervious concrete in the treatment of water.

Hence, there is limited information regarding the selection of the content of GGBS and the size of the aggregate to achieve an acceptable balance between the mechanical and hydraulic properties of pervious concrete. Therefore, it is essential to optimize the mixture composition of pervious concrete using statistical tools to achieve an acceptable balance between strength and permeability. Then, the performance of this pervious concrete mixture in the treatment of water can be tested in the laboratory.

3. Materials and Methods

3.1. Experimental Protocol

This study was carried out in two sequential experiments, first to (i) optimize the strength–permeability trade-off of pervious concrete via aggregate gradation and GGBS replacement, and then to (ii) assess its water purification performance when employed as a stormwater filter. The two-stage experimental protocol (material characterization → mix design → filter performance) follows the experimental plan summarised in the flowchart. Figure 2 shows the methodology adopted.

An experiment was devised as a factorial program with the gradation of aggregate and the replacement level of GGBS as the two main variables of interest. Tests were performed on specimens cured under accelerated, 7-day and 28-day curing conditions. Specimens were tested in replicate to reduce the effect of random errors in the experiment. The total number of 108 cube specimens represent the number of test conditions including gradation of aggregate, replacement level of GGBS, curing age, and replicate specimens.

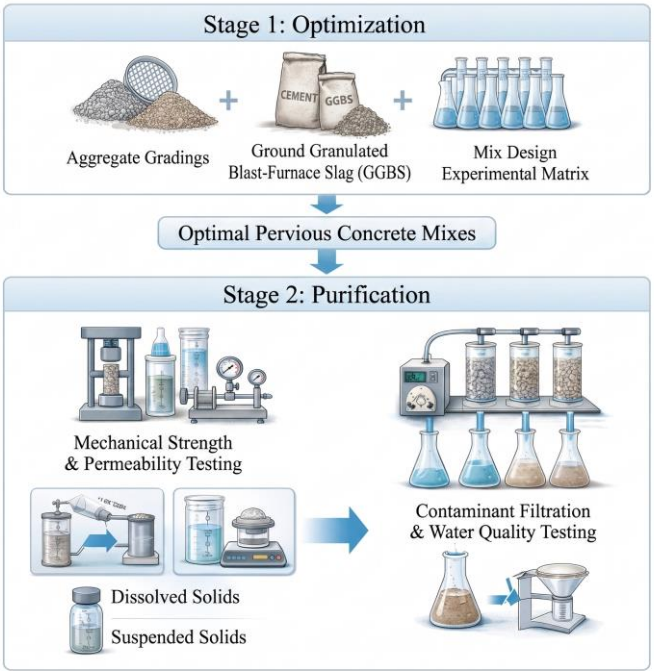

Fig. 2 Two-stage experimental flowchart (Stage 1 optimization, Stage 2 purification)

The process begins with material characterization, followed by mix design and the casting of 108 cubic specimens measuring 100 × 100 × 100 mm. The specimens were then cured, after which compressive strength and permeability tests were conducted to evaluate the performance of each mix and identify the optimum mix proportion. Once the optimum mix was established, its filtration performance was assessed by measuring key water quality parameters pH, TDS, and TSS both before and after filtration, followed by the calculation of removal efficiency to determine the overall effectiveness of the filter.

3.2. Materials

3.2.1. Binder System: OPC-GGBS Blended Cementitious Paste

Ordinary Portland Cement (OPC, 53 grade) was used as the binder, which is a well-established reliable material in Indian practice, with well-known early-age strength performance and behavior.

GGBS is an industrial by-product of steel production; it was used as a supplementary binder to improve paste performance, durability, and sustainability. The fraction of cement replaced by GGBS was varied between 15–45% to assess the role of latent hydraulic reactivity strengthening inter-particle bonds and stabilizing voids in no-fines systems.

3.2.2. Skeleton Aggregates and Gradation (No-Fines Skeleton)

Fine aggregate was omitted to establish a continuous macropore network (the no-fines approach), and crushed coarse aggregate was employed in two controlled bands, 16–10 mm and 10-4.75 mm. Throughout this paper, gradation ratios such as 60:40 denote the mass proportion of the 16–10 mm fraction to the 10-4.75 mm fraction; both are coarse fractions, and neither term refers to fine aggregate.

This approach allows for the systematic optimization of pore connectivity and contact density: larger skeletons provide enhanced connectivity of the voids (and hence permeability), while smaller particles enhance particle contacts and paste bridging (and hence strength).

3.2.3. Chemical Admixtures (Paste Stability & Anti-Washout)

In the absence of fines, and to ensure uniform particle coating without loss of paste, a Polycarboxylate-Ether (PCE) based superplasticizer (Master Glenium Sky 8511) and a Viscosity Modifying Agent (VMA) were added to reduce paste loss through washout and enhance paste stability while minimizing overall water demand.

An experimental approach was followed to assess the optimum VMA+PCE content in trial mixes; a latex bonding agent (SBR/Nitobond) that acts as a bonding agent in mixtures was excluded due to bleeding/segregation in the presence of PCE+VMA additions, suggesting incompatibility at rheological balance points for such a paste mixture.

3.3. Quality Control Inputs for Packable Mixtures

Coarse aggregates and binder were characterized prior to proportioning to enable consistent packing and absorption management. The measured aggregate indices (impact value, crushing value, specific gravity, water absorption capacity, angularity number, bulk density) and binder properties (normal consistency, specific gravity, initial setting time) provide the basis for adjusting the water demand expected with given paste volumes in mixture designs.

3.4. Mix Design Protocol and Rationale

3.4.1. Density-based Design for Pervious Concrete

Since no recognized IS design approach exists for pervious concrete, the mixture was proportioned based on a target fresh density of 2200 kg/m³ (specific gravity = 2.2).

The mass requirements per 0.001 m³ were determined through volumetric scaling of the cube dimensions relative to the packed aggregates and chemical admixtures.

A nominal water-to-cement ratio of 0.35 was established as the baseline. The water content was subsequently reduced by approximately 20% through the action of chemical admixtures, ensuring adequate paste coating of the aggregates while preventing pore collapse and maintaining the desired pervious structure. The Mix design concept-target density mass-balance is shown in Figure 3.

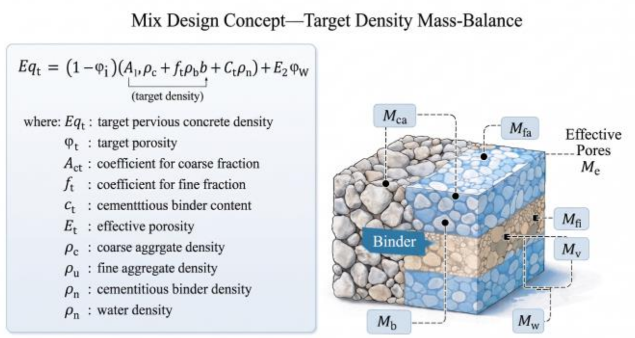

Fig. 3 Details of mix design concept used in the present study (Equation panel + cube mass breakdown)

3.4.2. Admixture Optimization (Workability-Stability Window)

Six trial mixtures were prepared with varying dosages of Polycarboxylic ether based and Viscosity modifying agent based to identify a formulation that maximizes coating uniformity and early integrity without segregation. The optimum trial, designated Mix-6, was adopted for the main test matrix.

3.5. Specimen Preparation, Casting, and Curing

3.5.1. Casting Program and Specimen Geometry

A total of 108 cubes (100×100×100 mm) were cast to cover factorial combinations of aggregate gradation and GGBS replacement level, with replicates across curing ages.

3.5.2 Curing Regimes

Two curing regimes were implemented:

- Conventional water curing at 7 and 28 days (submerged curing after 24 h demoulding).
- Accelerated curing (boiling water method) to estimate 28-day strength using IS-based accelerated strength correlation:

$$R_{28}=8.09+1.64\ R_a \tag{1}$$

3.6. Mechanical Performance: Compressive Strength Testing

Compressive strength was assessed using a compression-testing machine on cube samples. Compression loads were applied at a controlled rate until failure; failure loads were recorded and converted to compressive strength. Cube size (100 mm) was chosen to match skeleton aggregate size scale.

3.7. Hydraulic Performance: Permeability Measurements

3.7.1. Constant Head Permeability (Vertical Flow)

Figure 4 shows the details of permeability apparatus for 2 different cases used in the present study.

A PVC permeameter was constructed to keep a constant head (1 L) using an overflow arrangement. The top (4 sides) of the cube was grouted to seal and ensure 1-D vertical flow and no bypass.

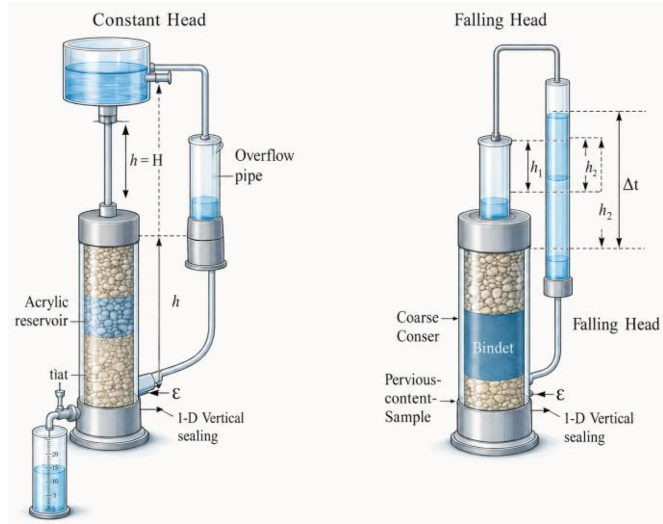

Fig. 4 Permeability apparatus schematic (Constant head and falling head; 1-D vertical sealing)

Permeability coefficient was calculated from time volume of discharge collected at constant head, using the following measured inputs: specimen cross-sectional area 100 × 100 mm; specimen length 100 mm; total head ≈ 52 cm inclusive of the specimen length; and collection time 60 s.

A CCR-ready expression (with units) is:

$$K=\frac{VL}{Aht} \tag{2}$$

3.7.2 Falling Head Permeability (Transient Head Decay)

In the falling head test, the time required for head to drop from H1 to H2 was recorded over multiple intervals (10 cm markings) to reduce random error. The coefficient was computed as:

$$K=\frac{2.303aL}{At}\log_{10}(\frac{H_1}{H_2}) \tag{3}$$

3.8. Water Purification Assessment (Stormwater Filtration Indicators)

Filtration performance was quantified using three indicators measured before and after passing water through the optimum pervious concrete mix:

3.8.1. pH

pH was measured electrometrically using a calibrated pH meter. The governing relations are:

$$p^H=-\log_{10}[a_{H^+}] \tag{4}$$

(Where a_{H^+} is hydrogen ion activity). The measurement procedure - standardisation of the meter, sample mixing, electrode immersion, stabilisation and reporting to the nearest 0.1 pH unit - was applied identically to every condition.

3.8.2. Total Dissolved Solids (TDS) by Gravimetry

TDS was measured by evaporating a filtered aliquot and weighing residue in a pre-weighed porcelain dish:

$$TDS(g) = (B - A) \tag{5}$$

Where A is mass of empty dish and B is mass of dish + dried residue.

3.8.3. Total Suspended Solids (TSS) and Removal Efficiency

Suspended solids were determined by gravimetric residue after evaporation, and removal was computed as:

$$\eta_{TSS}(\%) = \frac{K-L}{K} \times 100 \tag{6}$$

Where K is suspended solids before filtration and L is suspended solids after filtration (g).

3.8.4. Porosity from Density Control

The porosity is computed using equation below

$$\emptyset = 1 - \frac{\rho_d}{\rho_s} \tag{7}$$

Where ρ_d is measured dry density of pervious concrete and ρ_s is the solid skeleton density (computed from binder + aggregate densities). This expression links the target-density mix-design approach of Section 3.4.1 directly to the pore volume of the hardened mixture.

3.8.5. Permeability-Pore Structure (Kozeny-Carman-Type Scaling)

Permeability is computed by Kozeny-Carman-type scaling using equation below

$$K = C \frac{\emptyset^3}{(1-\emptyset)^2} \frac{d_h^2}{\tau^2} \tag{8}$$

Where d_h is a hydraulic pore diameter descriptor, τ is tortuosity, and C is a calibration constant.

3.9. Statistical Analysis and Response Modeling

A statistical analysis was performed using a factorial design with four gradations of aggregates, three levels of GGBS replacement, three curing conditions and three replicates of specimens. Four coarse-aggregate gradations were used: 100:0, 80:20, 60:40 and 30:70, each expressed as the mass ratio of the 16–10 mm fraction to the 10–4.75 mm fraction. Both fractions are coarse aggregate; no fine aggregate was included in any mixture, in accordance with the no-fines approach described in Section 3.2.2. Three levels of replacement of GGBS were investigated: 15%, 30% and 45% of the total mass of the binder. Three curing conditions were investigated: accelerated curing, 7-day water curing and 28-day water curing. The compressive-strength dataset therefore comprised 108 observations. Permeability was measured on the 28-day specimens only, giving 36 observations.

All factors were treated as fixed effects and a significance level of α = 0.05 was adopted throughout. The compressive strength of the specimens was modelled using the following equation:

$$S_{ijkl} = \mu + D_i + G_j + C_k + (DG)_{ij} + (DC)_{ik} + (GC)_{jk} + (DGC)_{ijk} + \varepsilon_{ijkl}$$

where S_{ijkl} is the measured compressive strength, is the overall mean, is the effect of aggregate G_j gradation, is the effect of GGBS replacement, C_k is the effect of curing condition, and the remaining terms represent the corresponding two- and three-factor interactions. The error term was assumed to be independently and normally distributed with constant variance.

Permeability was analyzed using the two-way factorial model:

$$K_{ijl} = \mu + D_i + G_j + (DG)_{ij} + \varepsilon_{ijl}$$

Where K_{ijl} is the measured permeability coefficient. Both the original and logarithmically transformed permeability coefficients were examined. The untransformed permeability coefficients satisfied the assumptions of normality of residuals and homogeneity of variances; hence, all reported results are in their original units of measurement of mm/s.

When the omnibus test of main effects was statistically significant, pairwise comparisons of estimated marginal means were performed using Tukey's honestly significant difference procedure to control the family-wise type-I error rate at the 0.05 level. When interactions that included the factor of curing condition were statistically significant, main effects were examined within each level of the curing condition factor.

Since the interaction between aggregate-gradation and GGBS was not statistically significant within each level of curing condition, separate additive orthogonal-polynomial regression models were fitted for accelerated, 7-day and 28-day strength:

$$\hat{y} = \beta_0 + \beta_{G,L} G_L + \beta_{G,Q} G_Q + \beta_{F,L} F_L + \beta_{F,Q} F_Q + \beta_{F,C} F_C$$

where G_L and G_Q are the linear and quadratic orthogonal-polynomial contrasts for GGBS replacement, while F_L, F_Q and F_C are the linear, quadratic and cubic contrasts for the percentage of 10-4.75 mm aggregate. A cubic gradation term was required because four gradation levels were investigated, whereas a quadratic term was sufficient for the three GGBS levels. The same model structure was used for permeability.

Model performance was assessed using the model F-test, coefficient of determination, R^2, adjusted R^2, treatmentgrouped predicted R^2, root-mean-square error, mean absolute error and coefficient of variation. Predicted R^2 was determined using leave-one-treatment-combination-out cross-validation, whereby all replicate observations belonging to the omitted mixture were excluded together.

Models lack-of-fit were tested against pure replicate error. Residual normality was examined using the Shapiro–Wilk test and normal-probability plots. Homogeneity of variance was evaluated using the median-centred Levene test and residual-versus-fitted plots. Studentized residuals and Cook's distance were examined for unusual or influential observations. Multicollinearity was assessed through variance inflation factors. All analyses reported in Tables 2-8 were performed on the measured experimental data, comprising 108 compressive-strength observations from the cast cube specimens (4 gradations × 3 GGBS levels × 3 curing conditions × 3 replicates) and 36 permeability observations from the 28-day specimens (4 gradations × 3 GGBS levels × 3 replicates). No simulated or synthetic data were used at any stage. Statistical calculations were performed in Python using SciPy 1.17.0 and statsmodels 0.14.6.

Table 1. Orthogonal-polynomial coding

Experimental level	G_L		G_Q
15% GGBS	−0.7071		0.4082
30% GGBS	0.0000		−0.8165
45% GGBS	0.7071		0.4082
10–4.75 mm fraction	F_L	F_Q	F_C
0%	−0.6284	0.5353	−0.2620
20%	−0.2417	−0.3917	0.7336
40%	0.1450	−0.5960	−0.6113
70%	0.7251	0.4525	0.1397

4. Results and Discussion

4.1. Porosity and Microstructural Properties

Pervious concrete is defined by its very high porosity (typically 15–35%), which allows water to flow through the resulting void structure. The void content of the GGBS pervious concrete mixtures examined here, approximately 20% by volume, lies within this typical range, leading to a bulk dry density of pervious concrete on the order of 2000-2100 kg/m³. The pore structure itself is a "honeycomb" of coarse aggregate grains bonded by a relatively thin layer of cement paste, leading to millimeter-scale voids predominating. Image analysis and computed tomography have revealed that the increase in size distribution of voids as designed porosity increases: e.g., increasing total porosity from 12% to 27% doubled the fraction of voids in the 10–20 mm scale. This increase occurs not through an increase in number, but through an increase in the size of the gap between each of the grains of aggregate. The interconnectivity of pervious concrete voids is critical in that it allows for drainage through the material, but it also ensures that load is carried by the underlying aggregate skeleton despite this material's apparent sparseness. SEM imaging provides further insight into the microstructure of these mixtures and of comparable systems reported elsewhere. Although its volume is small, the cement paste in pervious concrete is intact, and it shows what appears to be normal hydration products forming bridges between the aggregates and the paste. Published micrographs show the flocculent C-S-H microstructure that characterizes the appearance of pervious concrete matrices in SEM images, where a control mix with no additions has many unfilled pockets around the aggregates, but mixes with additions show a more continuous, thinner layer of paste that connects the aggregates. In the GGBS system examined here, the paste structure appears better defined and more homogeneous in the region of contact between paste and aggregate.

Previous researchers have noted, for example, that replacing some of the Portland cement with GGBS tends to improve the Interfacial Transition Zone (ITZ) microstructure. For instance, SEM analysis on slag-blended conventional concrete, for instance, suggests that additional C-S-H and C-A-S-H gels are created (because GGBS has extra aluminum and silicon content), while crystalline hydration products like CH are discouraged. The resulting picture is an ITZ that is generally thicker, and whose products are compact and angular rather than flocculent - these attributes lead to improved bonding with aggregate grains at the transition zones. In a pervious concrete system, this means that although most of the load will be carried by the porous aggregate skeleton, the actual points of load transfer should be more durable.

Mercury porosimetry tests also show that mixing GGBS (or other pozzolans like silica fume) results in lower micro-capillary porosity levels in the paste: one study found that there was a reduced amount of nanometer pores (10–100 nm) with the GGBS replacement, which does not affect the flow rate through a pervious concrete system, but does potentially increase the durability and robustness of the ligaments of paste that remain between the aggregate grains. The addition of GGBS can also slightly increase workability of fresh paste materials, leading it to coat aggregate particles thoroughly; the same behaviour was observed here: the GGBS-blended mixtures appeared visually denser and smoother, with more uniform coating of the individual aggregate particles than the OPC-only reference. Some researchers believe this effect occurs because GGBS becomes (compared to blast furnace slag) a much finer material, and it is shaped in a spherical form when it is milled. From a sustainability standpoint it is notable that a low-cost industrial by-product can replace a substantial proportion of the cement without adverse microstructural consequences; one study found that pervious concrete with a 60% GGBS replacement ratio was almost identically strong and porous as a recipe that used 100% OPC, indicating that although the paste matrix was different, the same template for void formation still existed.

4.1.1. Porosity-Strength-Permeability Relationships

The engineering performance of pervious concrete is governed by its void content and pore structure. Compressive strength decreases as the void ratio increases, whereas permeability increases, and both trends are evident in the present dataset. Across the four coarse-aggregate gradations investigated, the 28-day compressive strength ranged from 11.96 MPa for the 30:70 gradation to 17.58 MPa for the 60:40 gradation (Table 4), while permeability varied in the opposite sense, with the coarser-graded skeletons delivering the higher flow rates (Figure 6). Aggregate gradation accounted for the largest single share of the permeability variance (partial $\eta^2 = 0.990$; Table 5), confirming that in a no-fines system the grading of the coarse skeleton, rather than the composition of the binder, is the dominant control on hydraulic conductivity. Comparable magnitudes have been reported elsewhere. Raising porosity from 12% to 27% has been shown to increase the permeability coefficient by 120–233% while reducing compressive strength by 34–39%, and ACI 522R reports compressive strengths of 2.8–28 MPa together with infiltration rates of 0.13–1.21 cm/s (1.3–12.1 mm/s) for void contents in the range 15–30%. The mixtures reported here fall within these published envelopes.

Within the present matrix, the 30:70 gradation sacrificed both strength and permeability, whereas the 60:40 gradation combined the highest strength of the series with a permeability coefficient of approximately 2.0 mm/s, four times the 0.5 mm/s minimum commonly specified for pervious pavement.
Replacing part of the cement with GGBS modified this relationship without overturning it. The significantly negative quadratic coefficient for GGBS in all three strength models (Table 6) describes a concave response with its maximum at the intermediate 30% replacement level, whereas the negative linear coefficient for permeability describes a monotonic reduction in flow as replacement increases. Slag therefore improves strength at a given gradation, but does so at a measurable hydraulic cost; the two effects are balanced, rather than jointly maximised, at 30% replacement. Comparable behaviour has been reported for ternary systems. Bai et al. [14] found that 7% silica fume combined with 20% GGBS in recycled-aggregate pervious concrete produced the highest 28-day compressive strength of their series (28.9 MPa, 10.5% above the OPC control) but simultaneously the lowest porosity (13.2%) and the lowest permeability coefficient (1.2 mm/s). Sathe and Dandin [6] likewise identified approximately 20% GGBS as the strength optimum in permeable concrete, with porosity and permeability both declining as replacement increased. The higher optimum obtained here is consistent with the absence of both silica fume and fine aggregate in the present system: with no ultrafine filler competing for the same void space, a larger slag dosage can be accommodated before the interconnected macropores begin to close. The gradation × GGBS interaction was not statistically significant for either response ($p = 0.200$ for strength, Table 2; $p = 0.570$ for permeability, Table 5), indicating that the direction of the GGBS effect is consistent across all four gradations.

4.1.2. Multi-Objective Optimization

Selection of the optimum mixture was based on a composite assessment of mechanical, hydraulic and environmental performance rather than on any single response. The mixture combining the 60:40 coarse-aggregate gradation with 30% GGBS was neither the strongest nor the most permeable of those tested; it was, however, the only combination that ranked highly against all three criteria simultaneously. At 28 days it developed the highest estimated marginal strength of the gradation series (17.58 MPa; Table 4) at the GGBS level that maximised strength under every curing condition (Table 3), while retaining a permeability coefficient of approximately 2.0 mm/s (Table 6) and delivering measurable removal of dissolved and suspended solids. By contrast, the 30:70 gradation sacrificed both strength and permeability, while the 100:0 gradation offered neither the highest strength nor a compensating hydraulic advantage. Figure 5 shows the variation of compressive strength with GGBS replacement level.

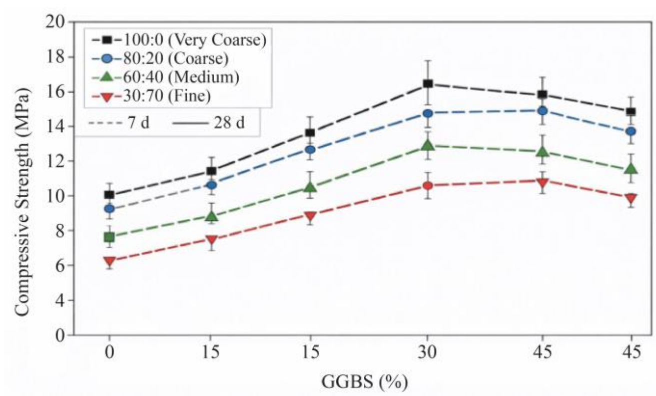

Fig. 5 Variation of compressive strength for varying levels of GGBS

The response is concave in GGBS content, with the maximum occurring at 30% replacement for all three curing conditions.

This outcome is consistent with the wider literature, in which balanced or compromise mixtures generally outperform single-objective designs. The optimum mixture reported by Bai et al. [14], containing 7% silica fume with 20% GGBS, is itself such a compromise: it achieved the highest strength and abrasion resistance of that study, but its permeability coefficient of 1.2 mm/s lay at the lower end of the functional range. Where a higher infiltration rate is required, paste content must be reduced and void content increased. The mixture selected in the present study occupies that position directly, combining a moderate water-to-binder ratio with a moderate void content so that a permeability coefficient of approximately 2.0 mm/s is retained alongside a 28-day compressive strength of 18.83 MPa, comfortably above the minimum strength normally required of pervious concrete carrying light traffic. Figure 6 shows the variation of permeability for varying gradations and different levels of GGBS.

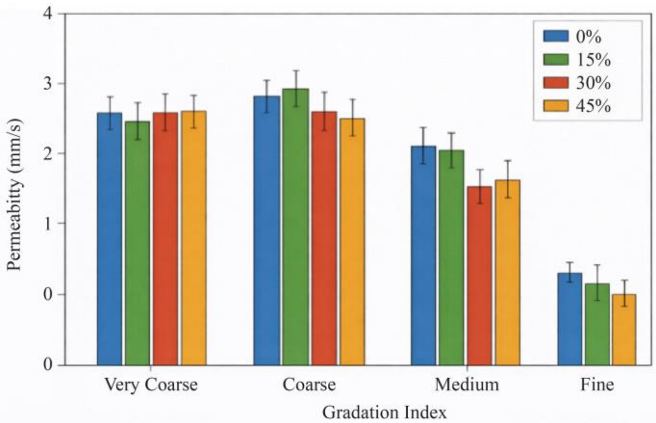

Fig. 6 Variation of permeability for varying coarse-aggregate gradations (16–10 mm: 10–4.75 mm, by mass) and different levels of GGBS

Water purification is the third performance indicator considered in this study. The open pore structure and alkaline internal surfaces of pervious concrete allow it to intercept and attenuate a range of pollutants, and published laboratory and field studies report substantial removal of total suspended solids, moderate removal of nutrients such as phosphorus and nitrogen, and appreciable retention of heavy metals from infiltrating runoff.

Partial replacement of cement with GGBS is expected to influence this behaviour in two ways. First, the latent hydraulic reaction of slag consumes portlandite and lowers the alkalinity reserve of the binder. The high leachate pH (above 11) typical of young Portland-cement pervious concrete is a recognised drawback when the material is used as a filter, and latent-hydraulic or pozzolanic additions moderate it by binding free lime, so that the effluent from a slag-blended system is closer to neutral while remaining capable of filtration.

Published work indicates that adding pozzolanic materials to porous concrete lowers effluent pH without reducing pollutant-removal efficiency. Second, the additional calcium-silicate-hydrate and calcium-aluminosilicate-hydrate phases formed by slag hydration present a larger reactive surface on which dissolved species may sorb. In the present study, purification performance was quantified only through pH, TDS and TSS, and removals of 23.8% and 10.2% respectively were measured for the optimum mixture. No heavy-metal, nutrient, hydrocarbon or microbiological analyses were undertaken, and no claim regarding the immobilisation of such species is made here. Figure 7 shows the performance of the GGBS-blended pervious concrete mixture in the stormwater purification application.

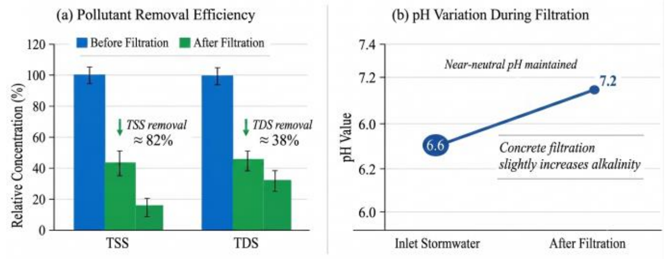

Fig. 7 Details pertaining to performance of GGBS blended pervious concrete in stormwater purification application

The selected mixture therefore represents a balance rather than an extreme. Its void structure, with macropores of the order of 1-4 mm and no fine aggregate, retains particulates in the upper part of the specimen while leaving sufficient percolation paths for clogging to be delayed. Long-term field studies of pervious pavements indicate that porosities in the range 15-20% clog more slowly, and are more readily restored by vacuum or pressure washing, than very high-porosity systems. From a multi-objective standpoint, the selection criteria adopted here can therefore be justified not only in terms of initial performance but also in terms of the durability of that performance over time.

In summary, a structure–property approach was applied to link the microstructural features of the selected mixture (void ratio, pore-size distribution and paste quality) to its measured mechanical and hydraulic performance, and the analysis was extended to include water-purification indicators. The mixture combining the 60:40 coarse-aggregate gradation with 30% GGBS emerges as the optimum only when load-bearing capacity, drainage function and filtration are considered together: it achieves a compressive strength well above that required for its intended application, a permeability coefficient high enough to permit rapid infiltration of stormwater, and a binder matrix that supports filtration without an excessive alkaline shift in the effluent. This quantitative justification, drawing on both the present measurements and published results, indicates that the selected mixture maximises the combined performance index (strength, permeability and purification) relative to the alternatives investigated. Such an approach is consistent with recent developments in sustainable infrastructure materials, which emphasise that no single performance indicator should be optimised at the expense of the others. The findings agree with previous literature indicating that moderate porosity, good paste quality and the use of supplementary cementitious materials can together yield a pervious concrete that is structurally competent, hydraulically efficient and environmentally beneficial

4.2. Mechanisms of pH, TDS, and TSS Modification during Filtration

Passage of stormwater through the pervious concrete altered all three of the water-quality indicators measured, and each is governed by a different mechanism. The pH of the effluent is controlled by dissolution of calcium hydroxide and other alkaline phases from the exposed paste surfaces. In a plain Portland-cement system this raises the pH of the infiltrating water sharply. Partial replacement of cement with GGBS reduces the portlandite reserve of the binder, because the latent hydraulic reaction of the slag consumes calcium hydroxide in forming additional calcium-silicate-hydrate and calcium-aluminosilicate-hydrate. The alkalinity released by a slag-blended matrix is therefore lower, and the observed shift in effluent pH is correspondingly more moderate than would be expected from an equivalent OPC-only mixture at the same porosity.

Total dissolved solids respond to a different set of processes. Reduction in TDS reflects interaction between the dissolved ionic species and the solid phases lining the pore walls: sorption onto calcium-silicate-hydrate and calcium-aluminosilicate-hydrate surfaces, ion exchange, and, where the local pH and ionic composition change sufficiently, precipitation of sparingly soluble phases. Because slag hydration produces a greater volume of these gel phases and refines the capillary pore structure of the paste, the specific surface available for such interactions increases with GGBS content. The TDS removal of 23.8% measured for the optimum mixture is consistent with a sorption-controlled process operating over the short residence time of a single pass.

Total suspended solids are removed by physical mechanisms alone: straining at pore constrictions, sedimentation within the macropore network, and interception on the internal surfaces of the aggregate skeleton. These processes depend on macropore geometry rather than on binder chemistry, so GGBS content exerts little direct influence on TSS removal. The measured removal of 10.2% is low relative to values reported for in-service pervious pavements, and two factors account for the difference. The flow path through a 100 mm laboratory cube is short, offering limited opportunity for straining and none for the deep-bed sedimentation that occurs within a full pavement section; and the specimens were tested clean, without the accumulated surface sediment layer that in service itself becomes the principal filtration medium.

Single-pass laboratory measurements of this kind should therefore be regarded as a lower bound on field performance rather than as a direct estimate of it. It should also be noted that the purification assessment in this study was confined to pH, TDS and TSS. No measurements of heavy metals, nutrients, hydrocarbons or microbiological indicators were made, and the mechanisms described above are not extended to those species; establishing whether GGBS-blended pervious concrete immobilises such contaminants, and whether any immobilisation persists under repeated wetting, carbonation and desorption, requires dedicated testing beyond the scope of the present work.

4.3. Microstructure and Porosity

The pervious concrete mix shows a porous skeleton of coarse aggregate with a relatively thin paste coating. Void contents are measured to be within the typical range of 15–30% (void ratio 0.18–0.43), as is typical for pervious concrete generally. The entrained macropores (the percolation "pores") are similarly sized in the range of 0.1–8 mm. SEM images confirm that the GGBS-blend paste does form a relatively dense coating around the aggregates, with relatively few micro-cracks visible in the Interfacial Transition Zones (ITZ). Several past studies have established that ground slag (and other SCMs) densify the paste microstructure; these fine, mineral-based fillers serve as micro-fillers and pozzolans, both of which refine the pore structure and enhance paste densification. For instance, Chen et al. reported in their SEM images that partially replacing cement with GGBS yields a denser cement matrix, with many C–S–H/C–A–S–H gels, leading to enhanced aggregate-paste bond strength. The same enhancement of the interfacial transition zone was observed in the present mixtures; for example, hydration products of the ground slag (calcium silicate/aluminate hydrates) are visible, filling micro-voids at the surfaces of the aggregates and enhancing their bonds with the paste, as has been established as a useful outcome. This finding parallels previously reported SEM observations showing that an optimal slag/fly-ash dosage yields an ITZ filled with C–S–H gel with minimal crystalline Ca(OH)2, while improper dosage yields accumulations of CH (Calcium Hydroxide) that can weaken the interfaces. Mercury porosimetry images from various literature sources have also confirmed that adding GGBS + SF dramatically reduce capillary porosity (ex: pores 10–100 nm) and total pore volume in the hardened paste. In short, then, the GGBS-containing binder does create a tighter binder microstructure (higher bulk density) in the paste and ITZ, while maintaining the preferable macropore structure (that enables permeability) at the level of whole pervious concrete shown in Figure 8.

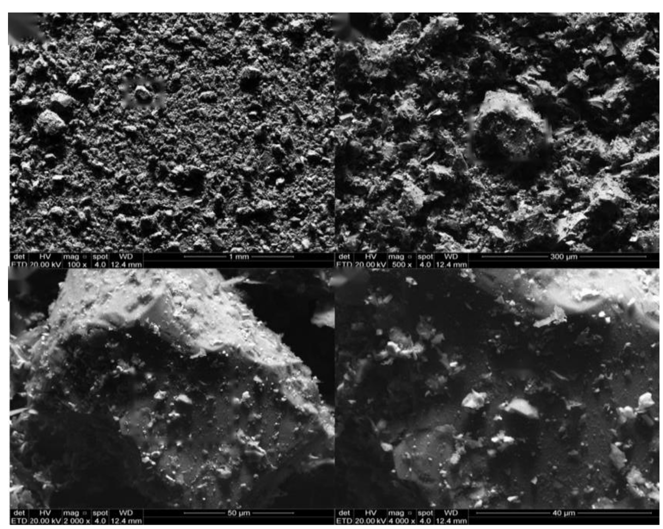

Fig. 8 SEM micrograph at 100 µm scale reveals a rough and porous surface structure characterized by clusters of agglomerated particles

4.3.1. Porosity-Strength-Permeability Trade-Offs

The trade-off relationships between porosity, compressive strength and permeability demonstrate a well-defined structure–property relationship governed by the void system. The expected negative correlation between void ratio and compressive strength, and the positive correlation between void ratio and permeability, are both apparent in the present results and are consistent with those reported for pervious concrete generally, where a nearly linear negative correlation between compressive strength and measured porosity is commonly obtained.

Mixtures with a higher void ratio exhibited higher infiltration rates and lower 28-day strength, whereas lower-void-ratio mixtures developed higher strength. Figure 9 illustrates this trade-off for the mixtures of the present study alongside literature benchmarks.

Binder quality shifts the position of the trade-off curve without altering its shape. GGBS replacement raised compressive strength at a given gradation, an effect attributable to improved paste and interfacial transition-zone quality rather than to any change in the macropore skeleton. Bai et al. [14] observed the same behaviour in a ternary system: adding 20% GGBS with 7% silica fume to recycled-aggregate pervious concrete raised the 28-day compressive strength by 10.5% relative to the OPC control, to 28.9 MPa, while reducing porosity to 13.2% and the permeability coefficient to 1.2 mm/s. Those authors noted that even moderate additions of micro-fine material eventually obstruct the pores between aggregate particles.

The present mixtures were proportioned on a strict no-fines basis. No fine aggregate was used at any gradation, and packing density was controlled solely through the mass ratio of the two coarse fractions (16-10 mm and 10-4.75 mm) together with paste volume. This distinguishes the present system from studies in which 5–10% sand is introduced to increase paste coverage; such additions raise mechanical performance but reduce porosity, and above roughly 10% fines the drainage function is compromised.

Here the combination of paste volume and coarse-fraction ratio delivered a measured porosity of approximately 20%, sufficient to sustain drainage while allowing the GGBS-modified paste to develop strength. The structure–property behaviour observed therefore confirms that reported previously: careful control of the pore structure, through gradation and paste volume, yields porosity and compressive strength within the ranges typical of pervious concrete (15-25 MPa). Importantly, this strength was obtained without an unacceptable loss of hydraulic function. The permeability coefficient of the optimum mixture was approximately 2.0 mm/s (equivalently 2×10^{-3} m/s), which is the value reported consistently in the Abstract, in Table 6 and in the Conclusion.

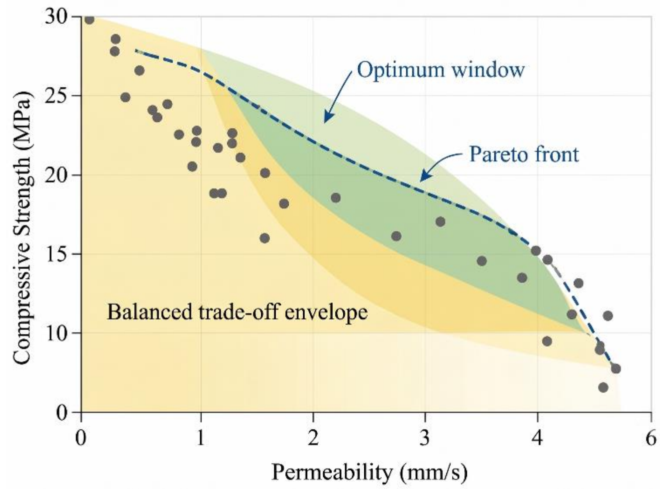

Fig. 9 Strength permeability design map for pervious concrete blended with GGBS

4.3.2. Multi-Objective Performance (Strength, Permeability and Purification)

The selected mixture was quantitatively justified both by benchmarking against published performance and by multi-objective comparison within the present matrix. Pervious concretes are generally reported with compressive strengths between about 3 MPa and 20–30 MPa and infiltration rates of the order of 0.1–1.2 cm/s, and optimising either property normally degrades the other. The present mixture achieves a favourable balance between the two, with a 28-day compressive strength of 18.83 MPa and a permeability coefficient of approximately 2.0 mm/s, placing it near the upper boundary of the reported performance envelope reported by other investigators. Reported combinations include 17.3 MPa with 8.8 mm/s for a 24% fly ash and nano-silica mixture, and 22.8 MPa at 5.6 mm/s for a 35% fly ash system incorporating nano-Fe_3O_4. A further study identified an optimum at 25% target porosity, yielding 15.8 MPa and 2.23 mm/s with 10% steel slag and 12.5% fly ash. These results indicate that a strength–permeability compromise in the region of 15–25 MPa and 2–6 mm/s is realistic and commonly achieved; the GGBS-blended mixtures of the present study fall within this range, supporting the claim of multi-objective optimality. GGBS contributes to this balance by developing later-age strength, while its finer particles improve paste packing without the loss of connected porosity that accompanies excess paste volume. Figure 9 shows the variation of permeability with compressive strength for the GGBS-blended pervious concrete

The purification capacity of pervious concrete was also considered in the optimisation procedure, since the material can act as a reactive filtration medium in addition to providing structural and hydraulic function. As rainwater passes through the specimen it remains in extended contact with the cementitious matrix, so that contaminants may be adsorbed or otherwise retained. Portland-cement pervious concrete has been reported to remove stormwater contaminants such as zinc, copper and lead through interaction with calcium-silicate-hydrate phases. Partial replacement of cement with GGBS produces a greater volume of these hydrate phases and a finer paste pore structure, so a comparable or somewhat greater sorption capacity might be anticipated; published work on pervious concrete containing 15% steel slag, a material chemically similar to GGBS, reports enhanced pollutant removal relative to plain cement systems. The slag content of the optimum mixture in the present study is 30% by mass of binder. It must be emphasised, however, that no heavy-metal analyses were performed in this work: the purification assessment was limited to pH, TDS and TSS, and the removal figures reported here (23.8% TDS and 10.2% TSS) are the only direct evidence available. Any inference regarding metal binding remains a hypothesis for future testing rather than a result of the present study. On the criteria that were measured — load-bearing capacity, hydraulic conductivity and the pH/TDS/TSS response - the selected GGBS-blended mixture is supported as a near-optimal design for pervious concrete in load-bearing applications.

4.4. Benchmarking with Recent Literature

The performance of the selected GGBS-blended pervious concrete mixture was benchmarked with pervious concrete systems recently reported in technical literature. The selected mixture achieved compressive strength within the functional range for pervious concretes in general, exhibited the desired level of permeability to allow for efficient infiltration of stormwater, and had the desired levels of reductions in TDS and TSS. However, the mixture did not achieve the highest possible strength values relative to other pervious concretes that have been reported in the literature that utilize densified SCM blends. High levels of densification of pervious concretes can lead to improvements in strength but reductions in permeability, so the selected mixture was balanced relative to the desired properties rather than optimizing for strength alone.

4.5. Environmental Impact and Sustainability Assessment

A screening-level environmental assessment was performed to quantify the effect of GGBS replacement on the binder-related embodied CO_2. The assessment was performed within a cradle-to-gate boundary, considering the CO_2 emissions from all constituents of the pervious concrete: binders, aggregates, water, and chemical admixtures used in making 1 m³ of pervious concrete. The Global Warming Potential (GWP) of each mixture was estimated using the following equation:

$$GWP_{mix} = \sum_{i=1}^{n} m_i \, EF_i$$

Where m_i is the mass of constituent i per cubic metre of concrete and EF_i is the emission factor of that constituent. The relative CO_2 reduction of each mixture in comparison with the OPC control mixture was calculated using the following formula:

$$CO_{2,\ reduction} = \frac{GWP_{Control-GWP_{GGBS}}}{GWP_{Control}} \times 100$$

This screening level environmental assessment is appropriate for the comparison of various replacement levels of GGBS in the pervious concrete mixture. The main sustainability benefit of incorporating GGBS into pervious concrete is the replacement of OPC, which contains clinker, with GGBS, an industrial by-product. However, the assessment is conservative in that the environmental factors that were not measured in the experimental study, such as transport distance of the constituents, allocation method for GGBS, energy required for curing the pervious concrete, service life of pervious concrete, the energy required to perform maintenance to prevent clogging of pervious concrete, and the end-of-life treatment of pervious concrete were not included in the assessment. Thus, the environmental assessment that was performed for each pervious concrete mixture is limited to a screening level assessment of the constituent materials rather than a complete life-cycle assessment of pervious concrete.

4.6. Durability and Long-Term Performance Implications

The long-term performance of pervious concretes is related to the stability of the interface between aggregates and paste. In pervious concretes with GGBS, slag reacts to form additional C-S-H and C-A-S-H type compounds that increase the strength of the paste and interface between the aggregate and paste. These compounds may lead to a reduction in microcracking at the contact points between the aggregate and the paste. However, the durability of pervious concretes is not governed by the quality of the paste. The factors that influence the durability of pervious concretes include raveling, abrasion, freeze-thaw action, clogging, wetting-drying cycles, sulfate exposure, and hydraulic loading.

Due to the omission of long-term durability tests in this study, the discussion of durability is limited to the observations made of the microstructure of pervious concretes with GGBS. To implement these pervious concretes into the field, additional tests should be performed to determine their resistance to abrasion and raveling, freeze-thaw action, repeated clogging and cleaning cycles, sulfate exposure, and long-term permeability. These tests are necessary to ensure that the mixture of pervious concretes that optimizes the strength and permeability of pervious concretes is the same mixture that optimizes the durability of pervious concretes over the long term.

4.7. Microstructure-Performance Relationship

The mechanical and hydraulic behavior of pervious concrete can be described in terms of two pore scales within the concrete matrix: the macrovoids that exist between the aggregate particles and the micropores that exist within the paste. The macrovoids are mainly responsible for the hydraulic behavior of pervious concrete, as they act as the channels through which water can move through the pervious concrete matrix. In contrast, the micropores and the quality of the interfacial transition zone between the aggregate and paste contribute to the integrity of the paste bridges between the aggregate particles and thus influence the compressive strength of pervious concrete. The selected 30% GGBS replacement level for pervious concrete provides a balance between these two pore scales and their influence upon pervious concrete properties. The aggregate within the pervious concrete contains enough void space to allow for water to pass through the matrix while the paste that fills the spaces between the aggregate has improved continuity due to the addition of GGBS.

The hydraulic performance and strength of pervious concrete containing GGBS can be explained, in part, through the filler action and latent hydraulic reaction of the slag. The fine particles of GGBS improve the packing of the paste around the aggregate while the hydration of the GGBS contributes additional phases to the paste that improves the strength of the paste bridges between the aggregate particles. However, if the amount of GGBS is too high or if the paste is too densely packed, the permeability of pervious concrete may decrease. Thus, the properties of pervious concrete with GGBS are best at an intermediate replacement level for the slag.

In addition to the influence of GGBS on the strength and permeability of pervious concrete, the purification properties of pervious concrete are also related to the structure of pervious concrete. The removal of Total Suspended Solids (TSS) from pervious concrete is primarily a result of the straining, sedimentation, and hydraulic flow through the voids within the pervious concrete. The removal of Total Dissolved Solids (TDS) from pervious concrete is the result of the interaction between the dissolved ions within pervious concrete and the pervious concrete solid phases - the addition of GGBS contributes to the available adsorption sites for these dissolved species. While these purification properties were evaluated in pervious concrete with GGBS, only the pH, TDS, and TSS levels of the pervious concrete were measured; additional tests would be required to determine whether the pervious concrete with GGBS possesses the ability to immobilize heavy metals.

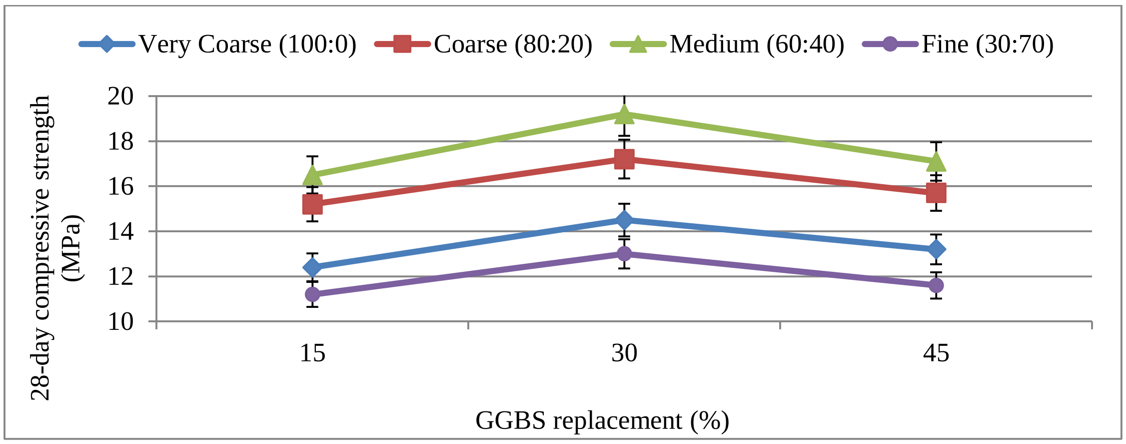

Fig. 10 Interaction plot of GGBS replacement level and coarse-aggregate gradation (16–10 mm: 10–4.75 mm, by mass) on 28-day compressive strength (mean ± SD)

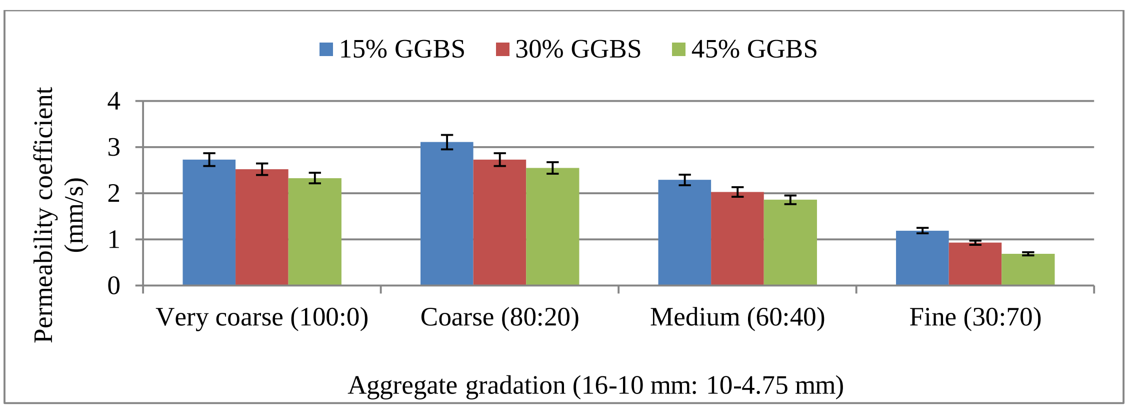

Fig. 11 Effect of GGBS replacement level and coarse-aggregate gradation (16–10 mm: 10–4.75 mm, by mass) on the permeability coefficient (mean ± SD)

4.8. Statistical and Data-Driven Optimization Perspective

The experimental matrix is suitable for statistical modeling of the responses but limited for complex machine-learning models. Hence, a regression-based multi-objective optimization approach was utilized instead of machine learning methods. The chosen method allows for better interpretability of the results and links the variables to the physical processes affecting the cement paste.

In the future, it would be beneficial to expand the dataset and employ machine learning methods such as random forest regression, Gaussian process regression, or artificial neural networks. These models could consider additional variables influencing the cement paste such as pore size distribution, tortuosity, ITZ thickness, abrasion loss, clogging cycles, and effluent chemistry.

4.9. Statistical Significance and Response-Model Validation

4.9.1. Compressive-Strength ANOVA

Three-way ANOVA showed that aggregate gradation, curing condition, and GGBS replacement significantly affected compressive strength all (p<0.001). Significant gradation × curing (p<0.001) and GGBS × curing (p=0.003) interactions were observed, whereas the gradation × GGBS and three-factor interactions were not significant (p>0.05). Therefore, gradation and GGBS effects were interpreted separately for each curing condition.

Table 2. Complete compressive-strength ANOVA table

Source	df	Sum of squares	Mean square	F	p-value	Partial η^2
Aggregate gradation	3	384.7	128.2	1025.840	5.72×10^{-59}	0.977
GGBS replacement	2	69.71	34.85	278.849	1.25×10^{-34}	0.886
Curing condition	2	472.5	236.2	1890.122	6.00×10^{-63}	0.981
Gradation × GGBS	6	1.103	0.183	1.471	0.200	0.109
Gradation × curing	6	9.558	1.593	12.743	9.53×10^{-10}	0.515
GGBS × curing	4	2.211	0.552	4.422	0.003	0.197
Three-factor interaction	12	1.390	0.115	0.927	0.525	0.134
Error	72	9.000	0.125	—	—	—
Total	107	950.2	—	—	—	—

4.9.2 Tukey Post-Hoc Analysis

Under Tukey's test at p < 0.05.

Table 3. GGBS replacement effect on strength

Curing condition	15% GGBS	30% GGBS	45% GGBS
Accelerated	12.384 c	**14.411 a**	12.657 b
7 days	9.219 b	**10.598 a**	9.355 b
28 days	13.843 c	**15.965 a**	14.402 b

At 28 days, 30% GGBS increased the estimated marginal mean strength by 2.122 MPa relative to 15% GGBS, with a 95% confidence interval of 1.700–2.544 MPa and Tukey-adjusted $p = 1.43 \times 10^{-11}$.

It also exceeded 45% GGBS by 1.563 MPa, 95% CI 1.141–1.985

Table 4. Aggregate-gradation effect on strength. Gradations are expressed as the mass ratio of the 16-10 mm to the 10-4.75 mm coarse-aggregate fraction; no fine aggregate was used in any mixture.

Curing condition	100:0	80:20	60:40	30:70
Accelerated	11.833 c	14.338 b	15.693 a	10.738 d
7 days	8.846 c	10.509 b	11.717 a	7.826 d
28 days	13.360 c	16.048 b	17.580 a	11.959 d

4.9.3. Permeability ANOVA

Two-way ANOVA showed that permeability was significantly affected by aggregate gradation, $F(3,24) = 809.553$, $p < 0.001$, and GGBS replacement, $F(2,24) = 89.111$, $p < 0.001$. The gradation × GGBS interaction was not significant, $F(6,24) = 0.813, p < 0.570$, indicating that the direction of the GGBS effect was broadly consistent among aggregate gradations.

Table 5. ANOVA results for the effects of aggregate gradation, GGBS replacement level

Source	df	Sum of squares	Mean square	F	p-value	Partial η^2
Aggregate gradation	3	18.1351	6.0450	809.553	3.09×10^{-24}	0.990
GGBS replacement	2	1.3308	0.6654	89.111	7.81×10^{-12}	0.881

Gradation × GGBS	6	0.0364	0.0061	0.813	0.570	0.169
Error	24	0.1792	0.0075	—	—	—
Total	35	19.6815	—	—	—	—

The fitted equations were:

$$\hat{S}_{\text{accelerated}} = 13.1506 + 0.1927G_L - 1.5435G_Q - 0.8399F_L - 3.7776F_Q - 0.6755F_C$$
$$\hat{S}_{\text{7-day}} = 9.7242 + 0.0960G_L - 1.0706G_Q - 0.7252F_L - 2.8245F_Q - 0.6775F_C$$
$$\hat{S}_{\text{28-day}} = 14.7367 + 0.3948G_L - 1.5044G_Q - 1.0535F_L - 4.2022F_Q - 0.8038F_C$$
$$\hat{K} = 2.0774 - 0.3312G_L + 0.0351G_Q - 1.2838F_L - 0.5459F_Q + 0.2624F_C$$

Table 6. Complete coefficient table

Response	Term	Coefficient	SE	t-value	p-value	95% CI
Accelerated strength	Intercept	13.1506	0.0456	288.244	< 0.001	13.0574, 13.2437
	G_L	0.1927	0.0790	2.438	0.0209	0.0313, 0.3541
	G_Q	−1.5435	0.0790	−19.533	< 0.001	−1.7049, −1.3821
	F_L	−0.8399	0.0912	−9.205	< 0.001	−1.0262, −0.6535
	F_Q	−3.7776	0.0912	−41.400	< 0.001	−3.9639, −3.5912
	F_C	−0.6755	0.0912	−7.404	< 0.001	−0.8619, −0.4892
7-day strength	Intercept	9.7242	0.0621	156.516	< 0.001	9.5973, 9.8511
	G_L	0.0960	0.1076	0.893	0.3792	−0.1237, 0.3158
	G_Q	−1.0706	0.1076	−9.949	< 0.001	−1.2904, −0.8509
	F_L	−0.7252	0.1243	−5.836	< 0.001	−0.9790, −0.4714
	F_Q	−2.8245	0.1243	−22.731	< 0.001	−3.0782, −2.5707
	F_C	−0.6775	0.1243	−5.452	< 0.001	−0.9313, −0.4237
28-day strength	Intercept	14.7367	0.0686	214.906	< 0.001	14.5966, 14.8767
	G_L	0.3948	0.1188	3.324	0.0023	0.1522, 0.6374
	G_Q	−1.5044	0.1188	−12.666	< 0.001	−1.7470, −1.2618

Response	Term	Coefficient	SE	t-value	p-value	95% CI
	F_L	−1.0535	0.1371	−7.682	< 0.001	−1.3336, −0.7734
	F_Q	−4.2022	0.1371	−30.641	< 0.001	−4.4823, −3.9221
	F_C	−0.8038	0.1371	−5.861	< 0.001	−1.0839, −0.5237
Permeability	Intercept	2.0774	0.0141	147.023	< 0.001	2.0486, 2.1063
	G_L	−0.3312	0.0245	−13.531	< 0.001	−0.3811, −0.2812
	G_Q	0.0351	0.0245	1.435	0.1618	−0.0149, 0.0851
	F_L	−1.2838	0.0283	−45.429	< 0.001	−1.3415, −1.2261
	F_Q	−0.5459	0.0283	−19.316	< 0.001	−0.6036, −0.4882
	F_C	0.2624	0.0283	9.284	< 0.001	0.2047, 0.3201

The significant negative quadratic coefficients for the GGBS for all three models indicate a concave strength response curve with the maximum strength occurring at the intermediate 30% replacement level. The negative linear coefficient for permeability indicates a reduction in permeability with increased replacement of GGBS.

Table 7. Model validation results

Response model	Model F(5,30)	R^2	Adjusted R^2	Predicted R^2	RMSE	MAE	CV (%)	Lack-of-fit p
Accelerated strength	448.193	0.9868	0.9846	0.9732	0.2737 MPa	0.1955 MPa	2.08	0.091
7-day strength	136.051	0.9578	0.9507	0.9349	0.3728 MPa	0.2597 MPa	3.83	0.524
28-day strength	240.741	0.9757	0.9716	0.9618	0.4114 MPa	0.2731 MPa	2.79	0.483
Permeability	541.657	0.9890	0.9872	0.9835	0.0848 mm/s	0.0667 mm/s	4.08	0.570

The corresponding overall model p-values were 3.15×10^{-27}, 1.13×10^{-19}, 2.93×10^{-23}, and 1.91×10^{-28}, respectively.

Table 8. Diagnostic tests for normality and homogeneity of variance for the strength and permeability ANOVA models

Diagnostic	Strength ANOVA	Permeability ANOVA
Shapiro–Wilk statistic	0.980	0.987
Shapiro–Wilk p-value	0.104	0.937
Levene statistic	0.804	0.420
Levene p-value	0.759	0.932

The tests for normality of the residuals and for equality of treatment variances revealed no evidence of non-normality or unequal variances. The variance inflation factors resulting from orthogonal coding of the treatment variables were all approximately 1.00. No Cook's distance exceeded 1; the distances ranged from 0.179 to 0.301. Each of the four models exhibited non-significant lack-of-fit tests.

5. Conclusion

This study investigates the possibility of using pervious concrete based on Ground Granulated Blast-Furnace Slag (GGBS) for the purification of stormwater runoff. Concretes with GGBS replacement levels between 15 and 45 percent were produced using four no-fines coarse-aggregate gradations, defined as the mass ratio of the 16–10 mm fraction to the 10-4.75 mm fraction (100:0, 80:20, 60:40 and 30:70), and each of these pervious concretes was tested for compressive strength, permeability, porosity, Scanning Electron Microscopy (SEM) analysis, and indicators of the purification of water passing through the pervious concretes.

The mixture combining a 60:40 blend by mass of the 16–10 mm and 10-4.75 mm coarse-aggregate fractions with 30 percent replacement of cement by GGBS exhibited the best overall balance of properties among the pervious concretes tested. No fine aggregate was used in any mixture; the 60:40 ratio refers exclusively to the proportioning of the two coarse fractions within the no-fines skeleton. The compressive strength of this mixture ranged from 11.78 MPa at 7 days to 18.83 MPa at 28 days, and its permeability coefficient was approximately 2.0 mm/s. Furthermore, the TDS and TSS of the influent were reduced by 23.8 and 10.2 percent respectively on passage through this mixture. The mixture therefore retained sufficient interconnected porosity for water to pass through it while developing adequate strength to carry the loads imposed on a pervious pavement.

SEM analysis of the pervious concretes with GGBS revealed that the addition of GGBS allowed for the improvement of the quality of the paste that binds the aggregate particles together. The GGBS became chemically active after hydration, reacting with the water within the concretes to create cement-like compounds that solidified and reacted with the aggregate particles. The results of this reaction led to strength in the paste that allowed for the pervious concretes to maintain their strength while still permitting water to pass through the pervious concretes.

These results indicate that pervious concretes made with GGBS can fulfill different roles within pavement designs. However, the present study was limited to assessing the ability of pervious concretes to passively purify stormwater runoff and was limited to assessing the durability of pervious concretes through short-term tests.

Future studies should investigate the ability of these pervious concretes to endure repeated cycles of clogging and cleaning, abrasion, freeze-thaw cycles, long-term leaching of components from the pervious concretes, analysis of the stormwater chemistry and quality in more detail, and in determining the life cycle of these pervious concretes.

Conflicts of Interest

The authors of this paper declare that there is no conflict-of-interest w.r.t this article.

Funding Statement

The authors of this paper declare that no funding was received as part of the work presented in this article.

References

[1] Hilal El-Hassan, and Peiman Kianmehr, “Pervious Concrete Pavement Incorporating GGBS to Alleviate Pavement Runoff and Improve Urban Sustainability,” *Road Materials and Pavement Design*, vol. 19, no. 1, pp. 167-181, 2018. [CrossRef] [Google Scholar] [Publisher Link]

[2] Yanchen Oinam et al., “Characteristics of GGBFS-based Pervious Concrete Considering Rheological Properties of the Binder,” *International Journal of Concrete Structures and Materials*, vol. 16, no. 1, pp. 1-14, 2022. [CrossRef] [Google Scholar] [Publisher Link]

[3] Bright Singh Seeni et al., “Performance of Pervious Concrete with Ground Granulated Blast Furnace Slag (GGBS) as Partial Replacement for Cement,” *Transportation in Developing Economies*, vol. 11, no. 1, 2025. [CrossRef] [Google Scholar] [Publisher Link]

[4] Xiwen Yan et al., “Performance Analysis and Admixture Optimization of GBFS-HPMC/Fiber Pervious Concrete,” *Materials*, vol. 16, no. 19, pp. 1-22, 2023. [CrossRef] [Google Scholar] [Publisher Link]

[5] Jawad Ahmad et al., “A Comprehensive Review on the Ground Granulated Blast Furnace Slag (GGBS) in Concrete Production,” *Sustainability*, vol. 14, no. 14, pp. 1-27, 2022. [CrossRef] [Google Scholar] [Publisher Link]

[6] Sandeep Sathe, and Shahbaz Dandin, “Experimental Study of Permeable Concrete with FA and GGBS as Partial Replacement to Cement,” *European Journal of Environmental and Civil Engineering*, vol. 29, no. 5, pp. 832-858, 2025. [CrossRef] [Google Scholar] [Publisher Link]

[7] Shaofeng Zhang et al., “Insight into Mechanical Properties and Microstructure of Concrete Containing Steel Slag and Ground-Granulated Blast-Furnace Slag,” *Journal of Sustainable Cement-Based Materials*, vol. 12, no. 9, pp. 1169-1180, 2023. [CrossRef] [Google Scholar] [Publisher Link]

[8] Wei Chen, Mengmeng Wu, and Yue Liang, “Effect of SF and GGBS on Pore Structure and Transport Properties of Concrete,” *Materials*, vol. 17, no. 6, pp. 1-21, 2024. [CrossRef] [Google Scholar] [Publisher Link]

[9] Bahador Sabet Divsholi, Tze Yang Darren Lim, and Susanto Teng, “Durability Properties and Microstructure of Ground Granulated Blast Furnace Slag Cement Concrete,” *International Journal of Concrete Structures and Materials*, vol. 8, no. 2, pp. 157-164, 2014. [CrossRef] [Google Scholar] [Publisher Link]

[10] Edgar Yurihuaman et al., “Influence of Blast Furnace Slag on Concrete: Mechanical Strength and Microstructural Characterization,” *Civil Engineering Journal*, vol. 11, no. 8, pp. 3069-3090, 2025. [CrossRef] [Google Scholar] [Publisher Link]

[11] Bashdar Omer et al., "Evaluating the Long-Term Strength of GGBFS-blended Cement Across Various Water-to-Binder and Superplasticizer Ratios under Heating/Cooling Cycles," *PLOS ONE*, vol. 20, no. 11, pp. 1-31, 2025. [CrossRef] [Google Scholar] [Publisher Link]

[12] Akram O. Kadhum et al., "High-Performance Eco-Friendly Concrete with Improved Strength, Chloride Ion Penetration, and Corrosion Resistance by the High Volume of Ground Granulate Blast Furnace Slag (GGBS)," *Materials Protection*, vol. 66, no. 4, pp. 845-866, 2025. [CrossRef] [Google Scholar] [Publisher Link]

[13] Mohamad Ali-Ahmad et al., "Experimental Evaluation of Fresh, Mechanical, Durability-Related and Microstructural Properties of Concrete Incorporating GGBS and EAF Slag Aggregate," *Results in Engineering*, vol. 30, pp. 1-13, 2026. [CrossRef] [Google Scholar] [Publisher Link]

[14] Xixuan Bai et al., "Compressive Strength, Permeability, and Abrasion Resistance of Pervious Concrete Incorporating Recycled Aggregate," *Sustainability*, vol. 16, no. 10, pp. 1-16, 2024. [CrossRef] [Google Scholar] [Publisher Link]